An Improved iUPQC Controller to Provide Additional Grid-Voltage Regulation as a STATCOM

Bruno W. França, *Student Member, IEEE*, Leonardo F. da Silva,
Maynara A. Aredes, *Student Member, IEEE*, and Maurício Aredes, *Member, IEEE*

Abstract—**This paper presents an improved controller for the dual topology of the unified power quality conditioner (iUPQC) extending its applicability in power-quality compensation, as well as in microgrid applications. By using this controller, beyond the conventional UPQC power quality features, including voltage sag/swell compensation, the iUPQC will also provide reactive power support to regulate not only the load-bus voltage but also the voltage at the grid-side bus. In other words, the iUPQC will work as a static synchronous compensator (STATCOM) at the grid side, while providing also the conventional UPQC compensations at the load or microgrid side. Experimental results are provided to verify the new functionality of the equipment.**

Index Terms—**iUPQC, microgrids, power quality, static synchronous compensator (STATCOM), unified power quality conditioner (UPQC).**

I. INTRODUCTION

CERTAINLY, power-electronics devices have brought about great technological improvements. However, the increasing number of power-electronics-driven loads used generally in the industry has brought about uncommon power-quality problems. In contrast, power-electronics-driven loads generally require ideal sinusoidal supply voltage in order to function properly, whereas they are the most responsible ones for abnormal harmonic currents level in the distribution system. In this scenario, devices that can mitigate these drawbacks have been developed over the years. Some of the solutions involve a flexible compensator, known as the unified power quality conditioner (UPQC) [1]–[7] and the static synchronous compensator (STATCOM) [8]–[13].

The power circuit of a UPQC consists of a combination of a shunt active filter and a series active filter connected in a back-to-back configuration. This combination allows the simultaneous compensation of the load current and the supply voltage, so that the compensated current drawn from the grid and the compensated supply voltage delivered to the load are kept balanced and sinusoidal. The dual topology of the UPQC, i.e., the iUPQC, was presented in [14]–[19], where the shunt active filter behaves as an ac-voltage source and the series one as an ac-current source, both at the fundamental frequency. This is a key point to better design the control gains, as well as to optimize the LCL filter of the power converters, which allows improving significantly the overall performance of the compensator [20].

The STATCOM has been used widely in transmission networks to regulate the voltage by means of dynamic reactive-power compensation. Nowadays, the STATCOM is largely used for voltage regulation [9], whereas the UPQC and the iUPQC have been selected as solution for more specific applications [21]. Moreover, these last ones are used only in particular cases, where their relatively high costs are justified by the power quality improvement it can provide, which would be unfeasible by using conventional solutions. By joining the extra functionality like a STATCOM in the iUPQC device, a wider scenario of applications can be reached, particularly in case of distributed generation in smart grids and as the coupling device in grid-tied microgrids.

In [16], the performance of the iUPQC and the UPQC was compared when working as UPQCs. The main difference between these compensators is the sort of source emulated by the series and shunt power converters. In the UPQC approach, the series converter is controlled as a nonsinusoidal voltage source and the shunt one as a nonsinusoidal current source. Hence, in real time, the UPQC controller has to determine and synthesize accurately the harmonic voltage and current to be compensated. On the other hand, in the iUPQC approach, the series converter behaves as a controlled sinusoidal current source and the shunt converter as a controlled sinusoidal voltage source. This means that it is not necessary to determine the harmonic voltage and current to be compensated, since the harmonic voltages appear naturally across the series current source and the harmonic currents flow naturally into the shunt voltage source.

In actual power converters, as the switching frequency increases, the power rate capability is reduced. Therefore, the iUPQC offers better solutions if compared with the UPQC in case of high-power applications, since the iUPQC compensating references are pure sinusoidal waveforms at the fundamental frequency. Moreover, the UPQC has higher switching losses due to its higher switching frequency.

Fig. 1. Example of applicability of iUPQC.

This paper proposes an improved controller, which expands the iUPQC functionalities. This improved version of iUPQC controller includes all functionalities of those previous ones, including the voltage regulation at the load-side bus, and now providing also voltage regulation at the grid-side bus, like a STATCOM to the grid. Experimental results are provided to validate the new controller design.

This paper is organized in five sections. After this introduction, in Section II, the iUPQC applicability is explained, as well as the novel feature of the proposed controller. Section III presents the proposed controller and an analysis of the power flow in steady state. Finally, Sections IV and V provide the experimental results and the conclusions, respectively.

II. EQUIPMENT APPLICABILITY

In order to clarify the applicability of the improved iUPQC controller, Fig. 1 depicts an electrical system with two buses in spotlight, i.e., bus A and bus B. Bus A is a critical bus of the power system that supplies sensitive loads and serves as point of coupling of a microgrid. Bus B is a bus of the microgrid, where nonlinear loads are connected, which requires premium-quality power supply. The voltages at buses A and B must be regulated, in order to properly supply the sensitive loads and the nonlinear loads. The effects caused by the harmonic currents drawn by the nonlinear loads should be mitigated, avoiding harmonic voltage propagation to bus A.

The use of a STATCOM to guarantee the voltage regulation at bus A is not enough because the harmonic currents drawn by the nonlinear loads are not mitigated. On the other hand, a UPQC or an iUPQC between bus A and bus B can compensate the harmonic currents of the nonlinear loads and compensate the voltage at bus B, in terms of voltage harmonics, unbalance, and sag/swell. Nevertheless, this is still not enough to guarantee the voltage regulation at bus A. Hence, to achieve all the desired goals, a STATCOM at bus A and a UPQC (or an iUPQC) between buses A and B should be employed. However, the costs of this solution would be unreasonably high.

An attractive solution would be the use of a modified iUPQC controller to provide also reactive power support to bus A, in addition to all those functionalities of this equipment, as presented in [16] and [18]. Note that the modified iUPQC serves as an intertie between buses A and B. Moreover, the microgrid connected to the bus B could be a complex system comprising distributed generation, energy management system, and other

Fig. 2. Modified iUPQC configuration.

control systems involving microgrid, as well as smart grid concepts [22]. In summary, the modified iUPQC can provide the following functionalities:

  a) "smart" circuit breaker as an intertie between the grid and the microgrid;
  b) energy and power flow control between the grid and the microgrid (imposed by a tertiary control layer for the microgrid);
  c) reactive power support at bus A of the power system;
  d) voltage/frequency support at bus B of the microgrid;
  e) harmonic voltage and current isolation between bus A and bus B (simultaneous grid-voltage and load-current active-filtering capability);
  f) voltage and current imbalance compensation.

The functionalities (d)–(f) previously listed were extensively explained and verified through simulations and experimental analysis [14]–[18], whereas the functionality (c) comprises the original contribution of the present work. Fig. 2 depicts, in detail, the connections and measurements of the iUPQC between bus A and bus B.

According to the conventional iUPQC controller, the shunt converter imposes a controlled sinusoidal voltage at bus B, which corresponds to the aforementioned functionality (d). As a result, the shunt converter has no further degree of freedom in terms of compensating active- or reactive-power variables to expand its functionality. On the other hand, the series converter of a conventional iUPQC uses only an active-power control variable $\bar{p}$, in order to synthesize a fundamental sinusoidal current drawn from bus A, corresponding to the active power demanded by bus B. If the dc link of the iUPQC has no large energy storage system or even no energy source, the control variable $\bar{p}$ also serves as an additional active-power reference to the series converter to keep the energy inside the dc link of the iUPQC balanced. In this case, the losses in the iUPQC and the active power supplied by the shunt converter must be quickly compensated in the form of an additional active power injected by the series converter into the bus B.

The iUPQC can serve as: a) "smart" circuit breaker and as b) power flow controller between the grid and the microgrid only if the compensating active- and reactive-power references
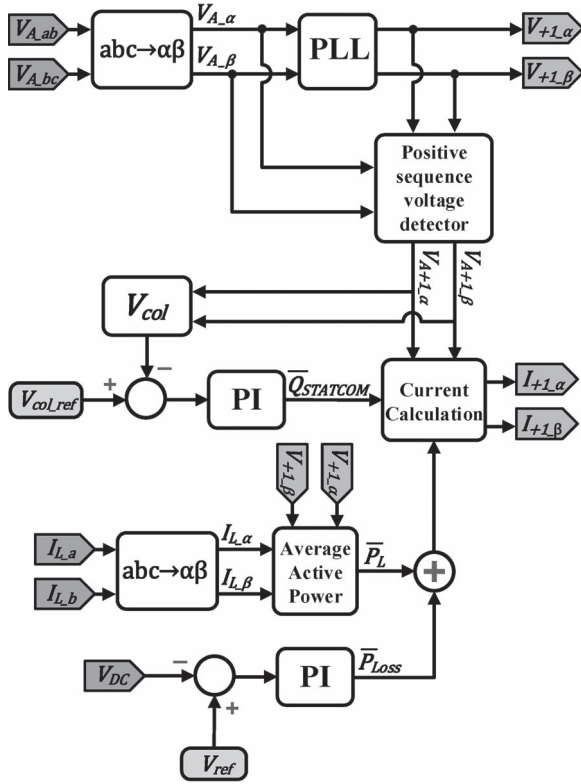
Fig. 3. Novel iUPQC controller.

of the series converter can be set arbitrarily. In this case, it is necessary to provide an energy source (or large energy storage) associated to the dc link of the iUPQC.

The last degree of freedom is represented by a reactive-power control variable $\overline{q}$ for the series converter of the iUPQC. In this way, the iUPQC will provide reactive-power compensation like a STATCOM to the bus A of the grid. As it will be confirmed, this functionality can be added into the controller without degrading all other functionalities of the iUPQC.

III. IMPROVED iUPQC CONTROLLER

A. Main Controller

Fig. 2 depicts the iUPQC hardware and the measured units of a three-phase three-wire system that are used in the controller. Fig. 3 shows the proposed controller. The controller inputs are the voltages at buses A and B, the current demanded by bus B (i_L), and the voltage v_{DC} of the common dc link. The outputs are the shunt-voltage reference and the series-current reference to the pulsewidth modulation (PWM) controllers. The voltage and current PWM controllers can be as simple as those employed in [18], or be improved further to better deal with voltage and current imbalance and harmonics [23]–[28].

First, the simplified Clark transformation is applied to the measured variables. As example of this transformation, the grid voltage in the $\alpha\beta$-reference frame can be calculated as

$$\begin{bmatrix} V_{A\_\alpha} \\ V_{A\_\beta} \end{bmatrix} = \begin{bmatrix} 1 & 1/2 \\ 0 & \sqrt{3}/2 \end{bmatrix} \begin{bmatrix} V_{A\_ab} \\ V_{A\_bc} \end{bmatrix}. \tag{1}$$

The shunt converter imposes the voltage at bus B. Thus, it is necessary to synthesize sinusoidal voltages with nominal ampli-

tude and frequency. Consequently, the signals sent to the PWM controller are the phase-locked loop (PLL) outputs with amplitude equal to 1 p.u. There are many possible PLL algorithms, which could be used in this case, as verified in [29]–[33].

In the original iUPQC approach as presented in [14], the shunt-converter voltage reference can be either the PLL outputs or the fundamental positive-sequence component V_{A+1} of the grid voltage (bus A in Fig. 2). The use of V_{A+1} in the controller is useful to minimize the circulating power through the series and shunt converters, under normal operation, while the amplitude of the grid voltage is within an acceptable range of magnitude. However, this is not the case here, in the modified iUPQC controller, since now the grid voltage will be also regulated by the modified iUPQC. In other words, both buses will be regulated independently to track their reference values.

The series converter synthesizes the current drawn from the grid bus (bus A). In the original approach of iUPQC, this current is calculated through the average active power required by the loads $\overline{P}_L$ plus the power $\overline{P}_{\text{Loss}}$. The load active power can be estimated by

$$P_L = V_{+1\_\alpha} \cdot i_{L\_\alpha} + V_{+1\_\beta} \cdot i_{L\_\beta} \tag{2}$$

where i_{L_α}, i_{L_β} are the load currents, and V_{+1_α}, V_{+1_β} are the voltage references for the shunt converter. A low-pass filter is used to obtain the average active power ($\overline{P}_L$).

The losses in the power converters and the circulating power to provide energy balance inside the iUPQC are calculated indirectly from the measurement of the dc-link voltage. In other words, the power signal $\overline{P}_{\text{Loss}}$ is determined by a proportional–integral (PI) controller (PI block in Fig. 3), by comparing the measured dc voltage V_{DC} with its reference value.

The additional control loop to provide voltage regulation like a STATCOM at the grid bus is represented by the control signal $\overline{Q}_{\text{STATCOM}}$ in Fig. 3. This control signal is obtained through a PI controller, in which the input variable is the error between the reference value and the actual aggregate voltage of the grid bus, given by

$$V_{\text{col}} = \sqrt{V_{A+1\_\alpha}^2 + V_{A+1\_\beta}^2}. \tag{3}$$

The sum of the power signals $\overline{P}_L$ and $\overline{P}_{\text{Loss}}$ composes the active-power control variable for the series converter of the iUPQC ($\overline{p}$) described in Section II. Likewise, $\overline{Q}_{\text{STATCOM}}$ is the reactive-power control variable $\overline{q}$. Thus, the current references $i_{+1\alpha}$ and $i_{+1\beta}$ of the series converter are determined by

$$\begin{bmatrix} i_{+1\_\alpha} \\ i_{+1\_\beta} \end{bmatrix} = \frac{1}{V_{A+1\_\alpha}^2 + V_{A+1\_\beta}^2} \begin{bmatrix} V_{A+1\_\alpha} & V_{A+1\_\beta} \\ V_{A+1\_\beta} & -V_{A+1\_\alpha} \end{bmatrix}$$
$$\times \begin{bmatrix} \overline{P}_L + \overline{P}_{\text{Loss}} \\ \overline{Q}_{\text{STATCOM}} \end{bmatrix}. \tag{4}$$

B. Power Flow in Steady State

The following procedure, based on the average power flow, is useful for estimating the power ratings of the iUPQC
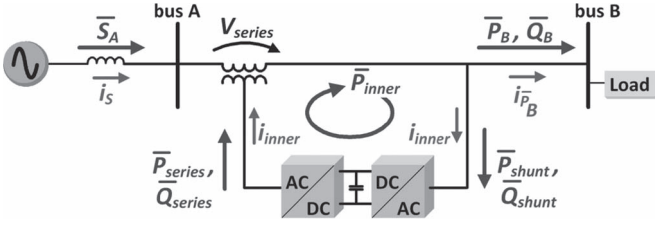
Fig. 4. iUPQC power flow in steady-state.

converters. For combined series–shunt power conditioners, such as the UPQC and the iUPQC, only the voltage sag/swell disturbance and the power factor (PF) compensation of the load produce a circulating average power through the power conditioners [34], [35]. According to Fig. 4, the compensation of a voltage sag/swell disturbance at bus B causes a positive-sequence voltage at the coupling transformer ($V_{\text{series}} \neq 0$), since $V_A \neq V_B$. Moreover, V_{series} and i_{P_B} in the coupling transformer leads to a circulating active power $\overline{P}_{\text{inner}}$ in the iUPQC. Additionally, the compensation of the load PF increases the current supplied by the shunt converter. The following analysis is valid for an iUPQC acting like a conventional UPQC or including the extra compensation like a STATCOM.

First, the circulating power will be calculated when the iUPQC is operating just like a conventional UPQC. Afterward, the equations will include the STATCOM functionality to the grid bus A. In both cases, it will be assumed that the iUPQC controller is able to force the shunt converter of the iUPQC to generate fundamental voltage always in phase with the grid voltage at bus A. For simplicity, the losses in the iUPQC will be neglected.

For the first case, the following average powers in steady state can be determined:

$$\overline{S}_A = \overline{P}_B \tag{5}$$

$$\overline{Q}_{\text{shunt}} = -\overline{Q}_B \tag{6}$$

$$\overline{Q}_{\text{series}} = \overline{Q}_A = 0 \text{ var} \tag{7}$$

$$\overline{P}_{\text{series}} = \overline{P}_{\text{shunt}} \tag{8}$$

where $\overline{S}_A$ and $\overline{Q}_A$ are the apparent and reactive power injected in the bus A; $\overline{P}_B$ and $\overline{Q}_B$ are the active and reactive power injected in the bus B; $\overline{P}_{\text{shunt}}$ and $\overline{Q}_{\text{shunt}}$ are the active and reactive power drained by the shunt converter; $\overline{P}_{\text{series}}$ and $\overline{Q}_{\text{series}}$ are the active and reactive power supplied by the series converter, respectively.

Equations (5) and (8) are derived from the constraint of keeping unitary the PF at bus A. In this case, the current passing through the series converter is responsible only for supplying the load active power, that is, it is in phase (or counterphase) with the voltages V_A and V_B. Thus, (7) can be stated. Consequently, the coherence of the power flow is ensured through (8).

If a voltage sag or swell occurs, $\overline{P}_{\text{series}}$ and $\overline{P}_{\text{shunt}}$ will not be zero, and thus, an inner-loop current (i_{inner}) will appear. The series and shunt converters and the aforementioned circulating active power ($\overline{P}_{\text{inner}}$) flow inside the equipment. It is conve-

nient to define the following sag/swell factor. Considering V_N as the nominal voltage

$$k_{\text{sag/swell}} = \frac{|\dot{V}_A|}{|\dot{V}_N|} = \frac{V_A}{V_N}. \tag{9}$$

From (5) and considering that the voltage at bus B is kept regulated, i.e., $V_B = V_N$, it follows that

$$\sqrt{3} \cdot k_{\text{sag/swell}} \cdot V_N \cdot i_S = \sqrt{3} \cdot V_N \cdot i_{P_B}$$

$$i_S = \frac{i_{P_B}}{k_{\text{sag/swell}}} = i_{\overline{P}_B} + i_{\text{inner}} \tag{10}$$

$$i_{\text{inner}} = \left| i_{P_B} \left(\frac{1}{K_{\text{sag/swell}} - 1} \right) \right|. \tag{11}$$

The circulating power is given by

$$\overline{P}_{\text{inner}} = \overline{P}_{\text{series}} = \overline{P}_{\text{shunt}} = 3(V_B - V_A)(i_{P_B} + i_{\text{inner}}). \tag{12}$$

From (11) and (12), it follows that

$$\overline{P}_{\text{inner}} = 3(V_N - V_A) \left(\frac{\overline{P}_B}{3V_N} \frac{1}{k_{\text{sag/swell}}} \right) \tag{13}$$

$$\overline{P}_{\text{inner}} = \overline{P}_{\text{series}} = \overline{P}_{\text{shunt}} = \frac{1 - K_{\text{sag/swell}}}{k_{\text{sag/swell}}} \overline{P}_B. \tag{14}$$

Thus, (14) demonstrates that $\overline{P}_{\text{inner}}$ depends on the active power of the load and the sag/swell voltage disturbance. In order to verify the effect on the power rate of the series and shunt converters, a full load system $\overline{S}_B = \sqrt{\overline{P}_B^2 + \overline{Q}_B^2} = 1$ p.u. with PF ranging from 0 to 1 was considered. It was also considered the sag/swell voltage disturbance at bus A ranging $k_{\text{sag/swell}}$ from 0.5 to 1.5. In this way, the power rating of the series and shunt converters are obtained through (6)–(8) and (14).

Fig. 5 depicts the apparent power of the series and shunt power converters. In these figures, the $k_{\text{sag/swell}}$-axis and the PF-axis are used to evaluate the power flow in the series and shunt power converters according to the sag/swell voltage disturbance and the load power consumption, respectively. The power flow in the series converter indicates that a high power is required in case of sag voltage disturbance with high active power load consumption. In this situation, an increased $\overline{P}_{\text{inner}}$ arises and high rated power converters are necessary to ensure the disturbance compensation. Moreover, in case of compensating sag/swell voltage disturbance with high reactive power load consumption, only the shunt converter has high power demand, since $\overline{P}_{\text{inner}}$ decreases. It is important to highlight that, for each PF value, the amplitude of the apparent power is the same for capacitive or inductive loads. In other words, Fig. 5 is the same for $\overline{Q}_B$ capacitive or inductive.

If the iUPQC performs all original UPQC functionalities together with the STATCOM functionality, the voltage at bus A is also regulated with the same phase and magnitude, that is, $\dot{V}_A = \dot{V}_B = \dot{V}_N$, and then, the positive sequence of the voltage
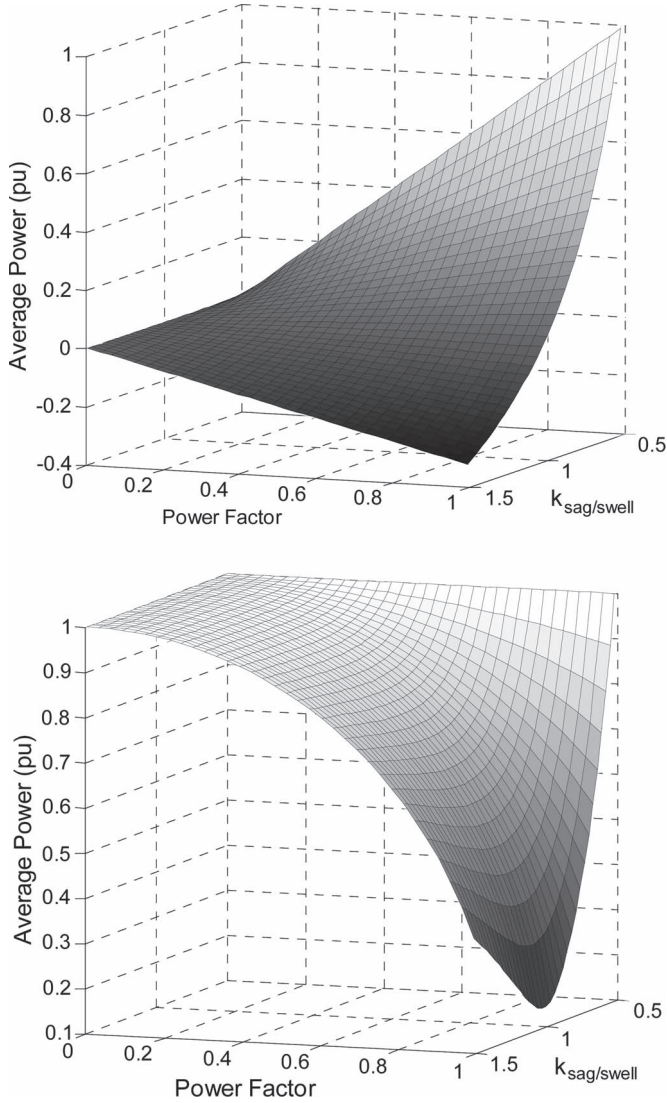
Fig. 5. Apparent power of the series and shunt converters, respectively.

TABLE I
iUPQC PROTOTYPE PARAMETERS

Parameter	Value
Voltage	220 V rms
Grid frequency	60 Hz
Power rate	5 kVA
DC-link voltage	450 V dc
DC-link capacitors	C = 9400 μF
Shunt converter passive filter	L = 750 μH R = 3.7 Ω C = 20.0 μF
Series converter passive filter	L = 1.0 mH R = 7.5 Ω C = 20.0 μF
Sampling frequency	19440 Hz
Switching frequency	9720 Hz
PI controller ($\overline{P}_{loss}$)	Kp = 4.0 Ki = 250.0
PI controller ($\overline{Q}_{STATCOM}$)	Kp = 0.5 Ki = 50.0
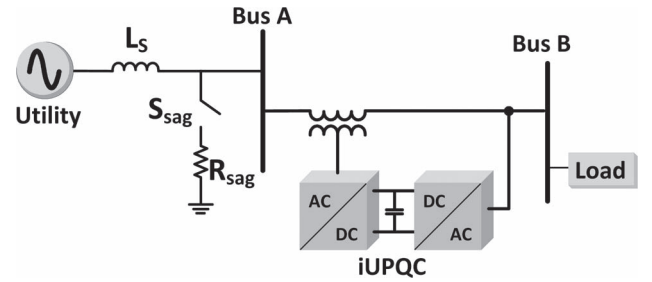
Fig. 6. iUPQC experimental scheme.

IV. EXPERIMENTAL RESULTS

at the coupling transformer is zero ($\overline{V}_{Series} = 0$). Thus, in steady state, the power flow is determined by

$$\overline{S}_A = \overline{P}_B + \overline{Q}_{STATCOM} \tag{15}$$

$$\overline{Q}_{STATCOM} + \overline{Q}_{series} = \overline{Q}_{shunt} + \overline{Q}_B \tag{16}$$

$$\overline{Q}_{series} = 0 \text{ var} \tag{17}$$

$$\overline{P}_{series} = \overline{P}_{inner} = 0 \text{ W} \tag{18}$$

where $\overline{Q}_{STATCOM}$ is the reactive power that provides voltage regulation at bus A. Ideally, the STATCOM functionality mitigates the inner-loop active power flow ($\overline{P}_{inner}$), and the power flow in the series converter is zero. Consequently, if the series converter is properly designed along with the coupling transformer to synthesize the controlled currents I_{+1_α} and I_{+1_β}, as shown in Fig. 3, then a lower power converter can be employed. Contrarily, the shunt converter still has to provide the full reactive power of the load and also to drain the reactive power injected by the series converter to regulate the voltage at bus A.

The improved iUPQC controller, as shown in Fig. 3, was verified in a 5-kVA prototype, whose parameters are presented in Table I. The controller was embedded in a fixed-point digital signal processor (TMS320F2812).

In order to verify all the power quality issues described in this paper, the iUPQC was connected to a grid with a voltage sag system, as depicted in Fig. 6. The voltage sag system was composed by an inductor (L_S), a resistor (R_{rmSag}), and a breaker (S_{Sag}). To cause a voltage sag at bus A, S_{Sag} is closed.

At first, the source voltage regulation was tested with no load connected to bus B. In this case, the iUPQC behaves as a STATCOM, and the breaker S_{Sag} is closed to cause the voltage sag.

To verify the grid-voltage regulation (see Fig. 7), the control of the $\overline{Q}_{STATCOM}$ variable is enabled to compose (4) at instant $t = 0$ s. In this experimental case, $L_S = 10$ mH, and $R_{Sag} = 7.5$ Ω. Before the $\overline{Q}_{STATCOM}$ variable is enabled, only the dc link and the voltage at bus B are regulated, and there is a voltage sag at bus A, as shown in Fig. 7. After $t = 0$ s, the iUPQC starts to draw reactive current from bus A, increasing the voltage until its reference value. As shown in Fig. 7, the load voltage at bus B is maintained regulated during all the time, and the grid-voltage regulation of bus A has a fast response.
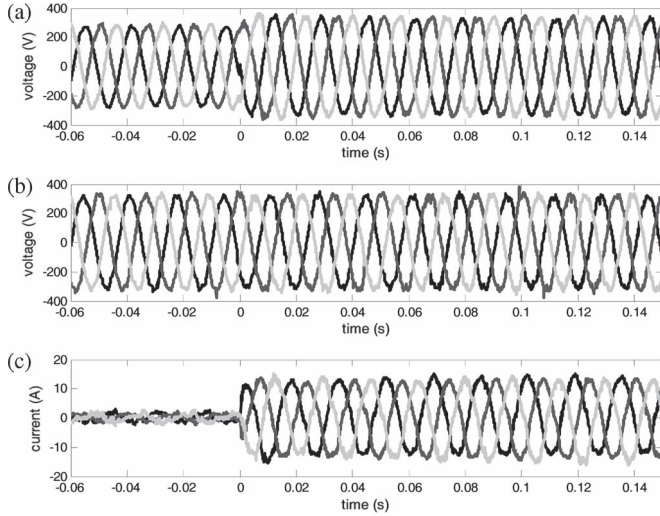
Fig. 7. iUPQC response at no load condition: (a) grid voltages V_A, (b) load voltages V_B, and (c) grid currents.
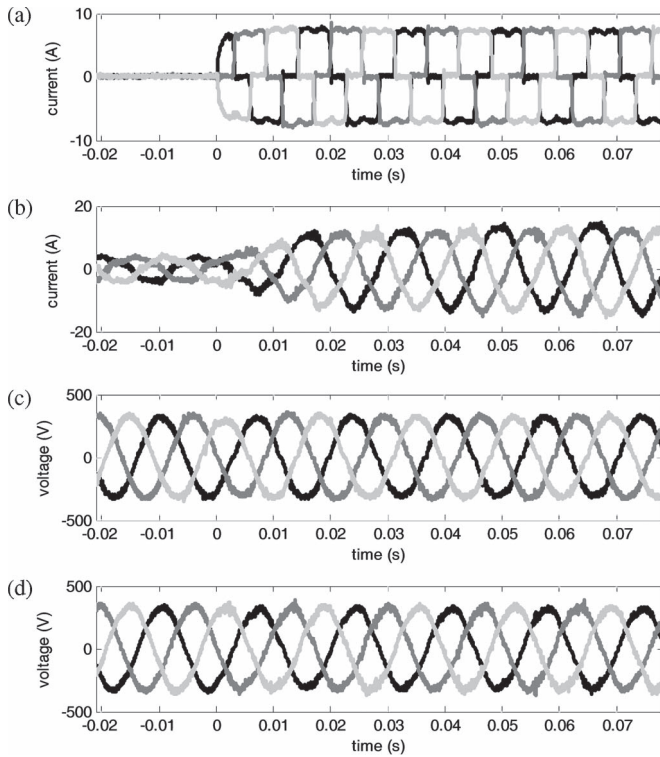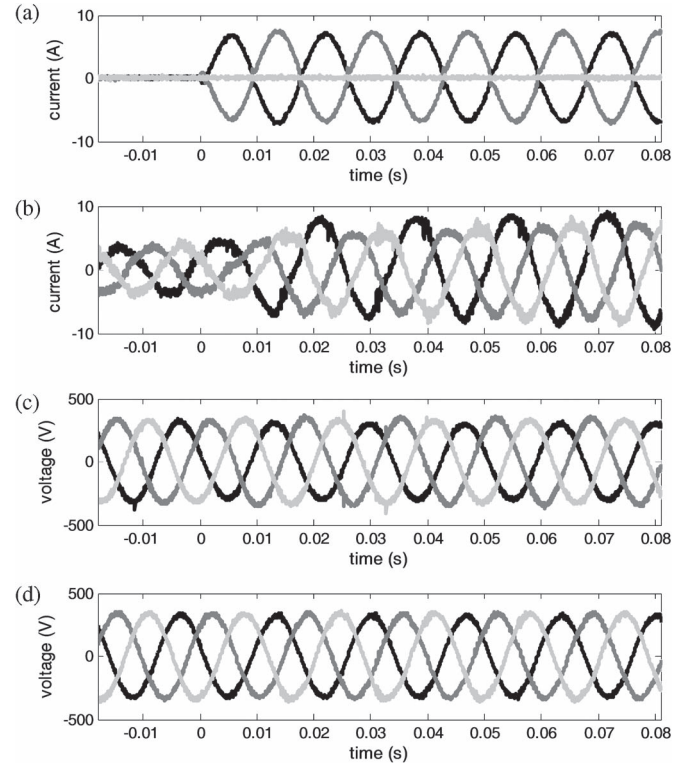

Fig. 8. iUPQC transitory response during the connection of a three-phase diode rectifier: (a) load currents, (b) grid currents, (c) load voltages and (d) grid voltages.

Next, the experimental case was carried out to verify the iUPQC performance during the connection of a nonlinear load with the iUPQC already in operation. The load is a three-phase diode rectifier with a series RL load at the dc link ($R = 45$ Ω and $L = 22$ mH), and the circuit breaker S_{Sag} is permanently closed, with a $L_S = 10$ mH and a $R_{\text{Sag}} = 15$ Ω. In this way, the voltage-sag disturbance is increased due to the load connection. In Fig. 8, it is possible to verify that the iUPQC is able to regulate the voltages at both sides of the iUPQC, simultaneously. Even after the load connection, at $t = 0$ s, the voltages are still regulated, and the currents drawn from bus A

Fig. 9. iUPQC transitory response during the connection of a two-phase diode rectifier: (a) load currents, (b) source currents, (c) load voltages, and (c) source voltages.

are almost sinusoidal. Hence, the iUPQC can perform all the power-quality compensations, as mentioned before, including the grid-voltage regulation. It is important to highlight that the grid-voltage regulation is also achieved by means of the improved iUPQC controller, as introduced in Section III.

Finally, the same procedure was performed with the connection of a two-phase diode rectifier, in order to better verify the mitigation of power quality issues. The diode rectifier has the same dc load ($R = 45$ Ω and $L = 22$ mH) and the same voltage sag ($L_S = 10$ mH and $R_{rmSag} = 15$ Ω). Fig. 9 depicts the transitory response of the load connection. Despite the two-phase load currents, after the load connection at $t = 0$ s, the three-phase current drained from the grid has a reduced unbalanced component. Likewise, the unbalance in the voltage at bus A is negligible. Unfortunately, the voltage at bus B has higher unbalance content. These components could be mitigated if the shunt compensator works as an ideal voltage source, i.e., if the filter inductor could be eliminated. In this case, the unbalanced current of the load could be supplied by the shunt converter, and the voltage at the bus B could be exactly the voltage synthesized by the shunt converter. Therefore, without filter inductor, there would be no unbalance voltage drop in it and the voltage at bus B would remain balanced. However, in a practical case, this inductor cannot be eliminated, and an improved PWM control to compensate voltage unbalances, as mentioned in Section III, is necessary.

V. CONCLUSION

In the improved iUPQC controller, the currents synthesized by the series converter are determined by the average active

power of the load and the active power to provide the dc-link voltage regulation, together with an average reactive power to regulate the grid-bus voltage. In this manner, in addition to all the power-quality compensation features of a conventional UPQC or an iUPQC, this improved controller also mimics a STATCOM to the grid bus. This new feature enhances the applicability of the iUPQC and provides new solutions in future scenarios involving smart grids and microgrids, including distributed generation and energy storage systems to better deal with the inherent variability of renewable resources such as solar and wind power.

Moreover, the improved iUPQC controller may justify the costs and promotes the iUPQC applicability in power quality issues of critical systems, where it is necessary not only an iUPQC or a STATCOM, but both, simultaneously. Despite the addition of one more power-quality compensation feature, the grid-voltage regulation reduces the inner-loop circulating power inside the iUPQC, which would allow lower power rating for the series converter.

The experimental results verified the improved iUPQC goals. The grid-voltage regulation was achieved with no load, as well as when supplying a three-phase nonlinear load. These results have demonstrated a suitable performance of voltage regulation at both sides of the iUPQC, even while compensating harmonic current and voltage imbalances.

REFERENCES

[1] K. Karanki, G. Geddada, M. K. Mishra, and B. K. Kumar, "A modified three-phase four-wire UPQC topology with reduced DC-link voltage rating," *IEEE Trans. Ind. Electron.*, vol. 60, no. 9, pp. 3555–3566, Sep. 2013.

[2] V. Khadkikar and A. Chandra, "A new control philosophy for a unified power quality conditioner (UPQC) to coordinate load-reactive power demand between shunt and series inverters," *IEEE Trans. Power Del.*, vol. 23, no. 4, pp. 2522–2534, Oct. 2008.

[3] K. H. Kwan, P. L. So, and Y. C. Chu, "An output regulation-based unified power quality conditioner with Kalman filters," *IEEE Trans. Ind. Electron.*, vol. 59, no. 11, pp. 4248–4262, Nov. 2012.

[4] A. Mokhtatpour and H. A. Shayanfar, "Power quality compensation as well as power flow control using of unified power quality conditioner," in *Proc. APPEEC*, 2011, pp. 1–4.

[5] J. A. Munoz *et al.*, "Design of a discrete-time linear control strategy for a multicell UPQC," *IEEE Trans. Ind. Electron.*, vol. 59, no. 10, pp. 3797–3807, Oct. 2012.

[6] V. Khadkikar and A. Chandra, "UPQC-S: A novel concept of simultaneous voltage sag/swell and load reactive power compensations utilizing series inverter of UPQC," *IEEE Trans. Power Electron.*, vol. 26, no. 9, pp. 2414–2425, Sep. 2011.

[7] V. Khadkikar, "Enhancing electric power quality using UPQC: A comprehensive overview," *IEEE Trans. Power Electron.*, vol. 27, no. 5, pp. 2284–2297, May 2012.

[8] L. G. B. Rolim, "Custom power interfaces for renewable energy sources," in *Proc. IEEE ISIE*, 2007, pp. 2673–2678.

[9] N. Voraphonpiput and S. Chatratana, "STATCOM analysis and controller design for power system voltage regulation," in *Proc. IEEE/PES Transmiss. Distrib. Conf. Exhib.—Asia Pac.*, 2005, pp. 1–6.

[10] J. J. Sanchez-Gasca, N. W. Miller, E. V. Larsen, A. Edris, and D. A. Bradshaw, "Potential benefits of STATCOM application to improve generation station performance," in *Proc. IEEE/PES Transmiss. Distrib. Conf. Expo.*, 2001, vol. 2, pp. 1123–1128.

[11] A. P. Jayam, N. K. Ardeshna, and B. H. Chowdhury, "Application of STATCOM for improved reliability of power grid containing a wind turbine," in *Proc. IEEE Power Energy Soc. Gen. Meet.—Convers. Del. Elect. Energy 21st Century*, 2008, pp. 1–7.

[12] C. A Sepulveda, J. A Munoz, J. R. Espinoza, M. E. Figueroa, and P. E. Melin, "All-on-chip dq-frame based D-STATCOM control implementation in a low-cost FPGA," *IEEE Trans. Ind. Electron.*, vol. 60, no. 2, pp. 659–669, Feb. 2013.

[13] B. Singh and S. R. Arya, "Back-propagation control algorithm for power quality improvement using DSTATCOM," *IEEE Trans. Ind. Electron.*, vol. 61, no. 3, pp. 1204–1212, Mar. 2014.

[14] M. Aredes and R. M. Fernandes, "A dual topology of unified power quality conditioner: The iUPQC," in *Proc. EPE Conf. Appl.*, 2009, pp. 1–10.

[15] M. Aredes and R. M. Fernandes, "A unified power quality conditioner with voltage sag/swell compensation capability," in *Proc. COBEP*, 2009, pp. 218–224.

[16] B. W. Franca and M. Aredes, "Comparisons between the UPQC and its dual topology (iUPQC) in dynamic response and steady-state," in *Proc. 37th IEEE IECON*, 2011, pp. 1232–1237.

[17] B. W. Franca, L. G. B. Rolim, and M. Aredes, "Frequency switching analysis of an iUPQC with hardware-in-the-loop development tool," in *Proc. 14th EPE Conf. Appl.*, 2011, pp. 1–6.

[18] B. W. Franca, L. F. da Silva, and M. Aredes, "Comparison between alpha-beta and DQ-PI controller applied to IUPQC operation," in *Proc. COBEP*, 2011, pp. 306–311.

[19] R. J. Millnitz dos Santos, M. Mezaroba, and J. C. da Cunha, "A dual unified power quality conditioner using a simplified control technique," in *Proc. COBEP*, 2011, pp. 486–493.

[20] Y. Tang *et al.*, "Generalized design of high performance shunt active power filter with output LCL filter," *IEEE Trans. Ind. Electron.*, vol. 59, no. 3, pp. 1443–1452, Mar. 2012.

[21] H. Akagi, E. Watanabe, and M. Aredes, *Instantaneous Power Theory and Applications to Power Conditioning*. New York, NY, USA: Wiley-IEEE Press, 2007.

[22] J. M. Guerrero, P. C. Loh, T.-L. Lee, and M. Chandorkar, "Advanced control architectures for intelligent microgrids—Part II: Power quality, energy storage, and AC/DC microgrids," *IEEE Trans. Ind. Electron.*, vol. 60, no. 4, pp. 1263–1270, Apr. 2013.

[23] S. R. Bowes and S. Grewal, "Novel harmonic elimination PWM control strategies for three-phase PWM inverters using space vector techniques," *Proc. Inst. Elect. Eng.—Elect. Power Appl.*, vol. 146, no. 5, pp. 495–514, Sep. 1999.

[24] M. Liserre, R. Teodorescu, and F. Blaabjerg, "Multiple harmonics control for three-phase grid converter systems with the use of PI-RES current controller in a rotating frame," *IEEE Trans. Power Electron.*, vol. 21, no. 3, pp. 836–841, May 2006.

[25] R. Teodorescu, F. Blaabjerg, U. Borup, and M. Liserre, "A new control structure for grid-connected LCL PV inverters with zero steady-state error and selective harmonic compensation," in *Proc. 19th Annu. APEC Expo.*, 2004, vol. 1, pp. 580–586.

[26] X. Yuan, W. Merk, H. Stemmler, and J. Allmeling, "Stationary-frame generalized integrators for current control of active power filters with zero steady-state error for current harmonics of concern under unbalanced and distorted operating conditions," *IEEE Trans. Ind. Appl.*, vol. 38, no. 2, pp. 523–532, Mar./Apr. 2002.

[27] D. N. Zmood and D. G. Holmes, "Stationary frame current regulation of PWM inverters with zero steady-state error," *IEEE Trans. Power Electron.*, vol. 18, no. 3, pp. 814–822, May 2003.

[28] D. N. Zmood, D. G. Holmes, and G. H. Bode, "Frequency-domain analysis of three-phase linear current regulators," *IEEE Trans. Ind. Appl.*, vol. 37, no. 2, pp. 601–610, Mar./Apr. 2001.

[29] M. Ciobotaru, R. Teodorescu, and F. Blaabjerg, "A new-single PLL structure based on second order generalized integrator," in *Proc. 37th IEEE PESC*, Jeju, Island, Korea, 2006, pp. 1–6.

[30] D. R. Costa, Jr., L. G. B. Rolim, and M. Aredes, "Analysis and software implementation of a robust synchronizing circuit based on pq theory," *IEEE Trans. Ind. Electron.*, vol. 53, no. 6, pp. 1919–1926, Dec. 2006.

[31] M.K. Ghartemani, "A novel three-phase magnitude-phase-locked loop system," *IEEE Trans. Circuits Syst. I, Reg. Papers*, vol. 53, no. 8, pp. 1798–1802, Aug. 2006.

[32] M. S. Padua, S. M. Deckmann, G. S. Sperandio, F. P. Marafao, and D. Colon, "Comparative analysis of synchronization algorithms based on PLL, RDFT and Kalman filter," in *Proc. IEEE ISIE*, Jun. 2007, pp. 964–970.

[33] J. A. Moor Neto, L. Lovisolo, B. W. França, and M. Aredes, "Robust positive-sequence detector algorithm," in *Proc. 35th IEEE IECON*, Nov. 2009, pp. 788–793.

[34] V. Khadkikar, A. Chandra, A. O. Barry, and T. D. Nguyen, "Steady state power flow analysis of unified power quality conditioner (UPQC)," in *Proc. ICIECA*, 2005, pp. 1–6.

[35] V. Khadkikar, A. Chandra, A. O. Barry, and T. D. Nguyen, "Conceptual study of unified power quality conditioner (UPQC)," in *Proc. IEEE Int. Symp. Ind. Electron.*, 2006, vol. 2, pp. 1088–1093.

Bruno W. França (S'14) was born in Rio de Janeiro, Brazil, in 1986. He received the B.Sc. and M.Sc. degrees in electrical engineering, in 2009 and 2012, respectively, from the Federal University of Rio de Janeiro (UFRJ), Rio de Janeiro, Brazil, where he is currently working toward the D.Sc. degree.

Since 2003, he has been involved in research projects with the Laboratory of Power Electronics and Medium-Voltage Applications (LEMT), Alberto Luiz Coimbra Institute for Graduate Studies and Research in Engineering (COPPE), UFRJ.

Maynara A. Aredes (S'14) was born in Rio de Janeiro, Brazil, in 1989. She is currently working toward the undergraduate degree in electrical engineering at the Federal University of Rio de Janeiro (UFRJ), Rio de Janeiro, Brazil.

She is currently a Researcher with the Laboratory of Power Electronics and Medium-Voltage Applications (LEMT), Alberto Luiz Coimbra Institute for Graduate Studies and Research in Engineering (COPPE), UFRJ.

Leonardo F. da Silva was born in Rio de Janeiro, Brazil. He received the Electrotechnical degree from the Escola Técnica Estadual (ETE) Ferreira Viana, Rio de Janeiro, Brazil. He is currently working toward the B.Sc. degree at the Universidade Estadual do Rio de Janeiro (UERJ), Rio de Janeiro, Brazil.

He is currently a Technical Researcher with the Laboratory of Power Electronics and Medium-Voltage Applications (LEMT), Alberto Luiz Coimbra Institute for Graduate Studies and Research in Engineering (COPPE), Federal University of Rio de Janeiro (UFRJ).

Maurício Aredes (M'96) received the Dr.Ing. degree from the Technische Universität Berlin, Berlin, Germany, in 1996.

Since 1997, he has been an Associate Professor with the Federal University of Rio de Janeiro (UFRJ), Rio de Janeiro, Brazil, where he teaches courses on power electronics. His current research interests include high-voltage dc and flexible ac transmission systems, active filters, renewable energy systems, and power quality issues.